

ABSTRACT

Title of Thesis: COMBINED LIQUEFACTION AND EXTRACTION OF BIOCRUDE
USING SUPERCRITICAL CARBON DIOXIDE

Joshua Schmidt
Master of Science, 2025

Thesis Directed by: Professor Ashwani Gupta
Department of Mechanical Engineering

The reliance on finite petroleum reserves, coupled with ever-increasing global energy demands, necessitates a concerted effort to develop sustainable liquid fuels. Given the inherent energy density advantage of liquid hydrocarbons, combustion engines will remain integral to the transportation sector for decades. This underscores the importance of advancing research into the liquefaction and extraction of biocrude from renewable feedstocks. However, scaling existing thermochemical processes is hampered by significant challenges concerning product separation, solvent recovery, and overall economic viability.

This thesis seeks to address these issues by investigating the innovative application of supercritical carbon dioxide (sCO₂) in a combined liquefaction and extraction system utilizing pinewood, an abundant lignocellulosic biomass resource. The experimental work utilized a novel integrated system for process intensification operated in the ranges of 250–350 °C and 200-300 bar. Feeding biomass between vessels at high-pressure was investigated using a mechanical feeder.

It was found that the combined process is limited by the extraction reaction, therefore rapid parameter screening was done via batch reactor setups. Critical process parameters investigated included temperature, CO₂ density, co-solvent, residence time, and the biomass-to-CO₂ ratio. Representative biocrude samples were analyzed using Gas Chromatography-Mass Spectrometry (GCMS). The analysis focused on identifying the presence and relative ratios of various detectable product species, including alkanes, esters, alcohols, and phenols.

The results confirmed that the biocrude derived from pinewood was rich in phenolic derivatives and aromatic hydrocarbons, characteristic products of lignin decomposition. To address liquefaction yield, this study demonstrated the effectiveness of a cosolvent system. A water and ethanol (50/50 wt%) cosolvent was introduced at a 5:1 combined solvent-to-biomass ratio. This improved yield from under 20% when only sCO₂ to above 60%, along with improved biomass conversion. This experimental work demonstrates that the integrated sCO₂ system, with the implementation of a polar cosolvent blend, offers a promising, scalable pathway to produce high-quality biocrude from lignocellulosic sources, directly supporting the long-term objective of offsetting petroleum dependency in the energy sector.

COMBINED LIQUEFACTION AND EXTRACTION OF BIOCRUDE USING
SUPERCRITICAL CARBON DIOXIDE

by

Joshua Schmidt

Thesis submitted to the Faculty of the Graduate School of the
University of Maryland, College Park in partial fulfillment
of the requirements for the degree of
Master of Science
2025

Advisory Committee:

Professor Ashwani Gupta, Chair

Professor Peter Sandborn

Professor Bao Yang

Copyright Notice

This work was supported by the U.S. Navy through the Civilian Institutions (CIVINS) Program under a full-time Duty Under Instruction billet at the University of Maryland. This publication is a work of the U.S. Government as defined in Title 17, United States Code, Section 101. Copyright protection is not available for this work in the United States.

Acknowledgments

I wish to acknowledge, with deep gratitude, the indispensable support I received throughout the thesis process. Firstly, I thank my advisor Dr. Ashwani Gupta for his support, mentorship, and guidance. I am extremely grateful he welcomed me to The Combustion Laboratory and I appreciate the time and thoughtfulness he invested in my intellectual development.

I am truly indebted to Dr. Kiran Burra for his daily guidance, expertise, and helpfulness. He is beyond instrumental in the progress of this work and provided unwavering support throughout my research. I am grateful to my colleague Vichaksha Ponnampereuma for his assistance and support.

I am humbled and thankful for the sacrifices my wife and children made to support the time dedicated to my studies.

I appreciate the opportunity to pursue this degree and the funding provided by the U.S. Navy through the Civilian Institutions (CIVINS) Program and for the oversight provided by the Naval Postgraduate School.

Finally, this material is based upon work supported by the U.S. Department of Energy's Office of Energy Efficiency and Renewable Energy (EERE) under the Bioenergy Technologies Office Award Number DE-EE0009757. Their support is gratefully acknowledged.

Neither the United States Government nor any agency thereof, nor any of their employees, makes any warranty, express or implied, or assumes any legal liability or responsibility for the accuracy, completeness, or usefulness of any information, apparatus, product, or process disclosed, or represents that its use would not infringe privately owned rights. Reference herein to any

specific commercial product, process, or service by trade name, trademark, manufacturer, or otherwise does not necessarily constitute or imply its endorsement, recommendation, or favoring by the United States Government or any agency thereof. The views and opinions expressed herein do not necessarily state or reflect those of the United States Government or any agency thereof.

Professional Publications:

K. G. Burra, J. Schmidt, V. Ponnampereuma, and A. K. Gupta, "Integrated Liquefaction-Extraction of Biomass for High-Quality Biocrude Production," *ASME 2025 International Mechanical Engineering Congress and Exposition (IMECE2025)*, Nov. 16–20, 2025, Memphis, TN, USA, Paper IMECE2025-165501.

Table of Contents

Acknowledgments	ii
Table of Contents.....	iv
List of Tables	v
List of Figures.....	vi
List of Abbreviations	vii
Chapter 1: Introduction.....	1
1.1 U.S. Energy.....	1
1.2 Biocrude.....	2
1.3 Biomass.....	3
1.4 Heating and Cooling rate	5
1.5 Temperature and Residence Time.....	5
1.6 Near-critical Liquefaction Extraction (NILE) in sCO ₂	6
Chapter 2: Materials and Equipment	8
2.1 Materials	8
2.2 Equipment.....	9
2.2.1 Reactor.....	9
2.2.2 Reactor Stirrers	9
2.2.3 Feeder	11
2.2.4 Collector (light fractions).....	11
2.2.5 Extractor (heavy fractions).....	12
2.2.6 Automatic Back Pressure Regulator (ABPR).....	12
2.2.7 Heater.....	12
2.2.8 CO ₂ supply and pump	12
2.2.9 Fully assembled test apparatus.....	13
Chapter 3: Procedures.....	16
3.1 Concurrent liquefaction and extraction	16
3.2 Batch Reactions	17
3.3 Acetone Extraction.....	18
3.4 sCO ₂ Extraction	19
3.5 Process Flow	20
Chapter 4: Results.....	22
4.1 Biocrude Yield.....	22
4.2 Composition of oil product	27
4.3 Cosolvent introduction.....	32
Chapter 5: Conclusions and Future Work.....	34
References	36

List of Tables

TABLE I: Mass Fraction of INL Pinewood	8
--	---

List of Figures

Fig. 1 U.S. Energy Consumption in 2023 provided by Lawrence Livermore National Laboratory [1]	1
Fig. 2 Lignin Structure [10]	4
Fig. 3 Various Hydrofaction™ reactions depending on time and temperature [3]	5
Fig. 4 Impact of temperature and residence time [11]	6
Fig. 5 Reactor Stirrers. (a) Paddle based. (b) Paint mixer based. (c) Counterrotating fans.	10
Fig. 6 Combined liquefaction-extraction, before addition of heated base. (1) Reactor. (2) Feeder. (3) Reactor stirrer motor. (4) Cooling fan. (5) Movable feeder gantry. (6) Extraction vessel. (7) ABPR. (8) Collector vessel. (9) CO ₂ pump	14
Fig. 7 Reactor with heated base plate added.....	15
Fig. 8 Feeder and reactor connected with 3/8 in high pressure tubing.....	15
Fig. 9 Rotary Evaporator.....	19
Fig. 10 Process flow diagram for integrated liquefaction-extraction.....	20
Fig. 11 Oil (biocrude) yields.....	22
Fig. 12 Total liquids yields	23
Fig. 13 Combined gas yields and losses. These values are calculated by subtraction of solids and liquids.	23
Fig. 14 Solid residue yields.....	24
Fig. 15 Representative liquid extracts showing oils and aqueous products	25
Fig. 16 Immersion cooling test using ice water bath	26
Fig. 17 High aqueous product yield from argon only environment.....	27
Fig. 18 Full plot of Total Ion Chromatogram, upper samples is 30 min and lower sample is 120 min residence time.	28
Fig. 19 Total Ion Chromatogram for retention times between 21-37 min, upper samples is 30 min and lower sample is 120 min residence time	29
Fig. 20 Total Ion Chromatogram for retention times between 37-52 min, upper samples is 30 min and lower sample is 120 min residence time	29
Fig. 21 Total Ion Chromatogram for retention times between 52-72 min, upper samples is 30 min and lower sample is 120 min residence time	30
Fig. 22 Total Ion Chromatogram for retention times between 65-84 min, upper samples is 30 min and lower sample is 120 min residence time	30
Fig. 23 Relative Area of Selected Compounds	31

List of Abbreviations

ABPR	Automatic Back Pressure Regulator
CIVINS	Civilian Institutions
CO ₂	Carbon Dioxide
EERE	Office of Energy Efficiency and Renewable Energy
GCMS	Gas Chromatography-Mass Spectrometry
IMECE2025	International Mechanical Engineering Congress and Exposition 2025
INL	Idaho National Laboratory
NILE	Near-Critical Liquefaction Extraction
NIST	National Institute of Standards and Technology
PID	Proportional-Integral-Derivative
PTFE	Polytetrafluoroethylene
SAF	Sustainable Aviation Fuels
sCO ₂	Supercritical Carbon Dioxide
wt%	Weight Percent

Chapter 1: Introduction

1.1 U.S. Energy

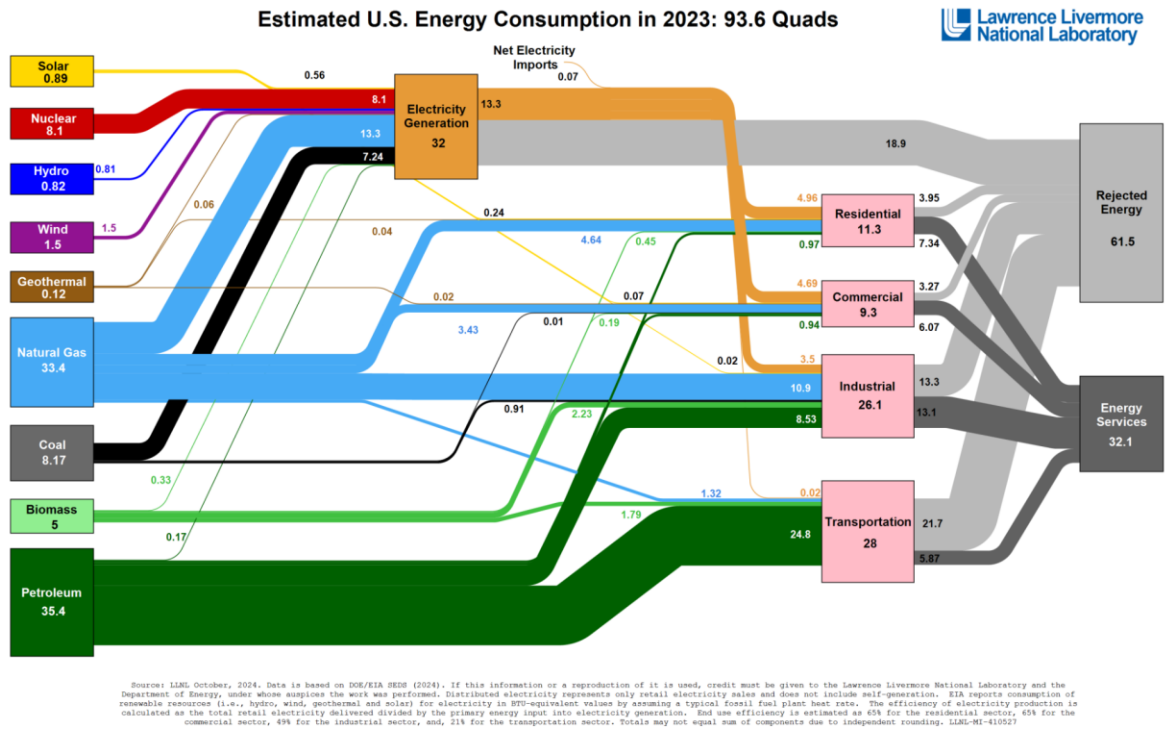


Fig. 1 U.S. Energy Consumption in 2023 provided by Lawrence Livermore National Laboratory [1]

The dominance of petroleum and the transportation sector on the national energy use is clearly demonstrated in the data compiled by Lawrence Livermore National Laboratory. Transportation represents the largest single sector input of energy use, accounting for 28 Quads in 2023 or roughly 37.5%. Petroleum supply was 35.4 Quads or 37.8% of the total national energy consumption. Biomass is a non-negligible contribution, but at 5 Quads is a seventh of the petroleum scale [1]. That biomass contribution as of 2023 is dominated by ethanol additives for gasoline and biodiesel products along with industrial wood uses. A significant contribution to greenhouse gas emissions, the extraction of petroleum products represents an opportunity to mitigate carbon emissions even if the delivered energy is still combusted hydrocarbons [2].

Because liquid fuels have high energy densities, the transportation section will continue to rely on this storage mechanism for decades [2]. In particular, the aviation industry must balance mounting pressure to mitigate carbon emissions in the face of global warming with massive infrastructure and technology overhauls that are prohibitively costly and time-consuming. Viable, which includes economical, Sustainable Aviation Fuels (SAF) must be developed in the near term [2].

1.2 Biocrude

Many alternatives to petroleum based liquid fuels have been presented, including syngas, iso-alkanes, cycloalkanes. The production of these alternatives currently relies primarily on the hydroprocessing of lipids and fatty acids sourced from specialized energy crops (e.g., soy and jatropha) or waste materials to yield a hydrocarbon stream. The second and equally significant route utilizes saccharide conversion, where sugars and cellulosic materials are processed into intermediate molecules, notably ethanol, for subsequent upgrading into drop-in jet fuel [2]. The advantages of biocrude have been a focused area of research. Biocrude is a subset of biofuels which include solid, liquid, and gaseous fuels sourced from biomass. Biocrude is generally a liquid fuel source that requires further refinement such as the process used to transition natural crude oil to a commercially viable product.

Biocrude can provide a renewable, domestically sourced, carbon-reducing pathway. Critically, it can be compatible with existing petroleum refinement processes, something close to a drop-in replacement for petroleum [3]. Thus, much work has been done to investigate the production of biocrudes.

Biocrudes are generally produced via fast pyrolysis and hydrothermal liquefaction. Fast pyrolysis does not require high pressure but does need dry biomass and requires higher temperatures for the reaction [4]. Hydrothermal liquefaction requires high pressure but can ingest

wet biomass and generally results in higher quality biocrude [5]. Other methods include gasification, the highest temperature process wherein the resulting gasses are condensed into liquid fuels [6]. Lastly, hydrothermal carbonization is a lower-temperature wet process that focuses on solid fuel production rather than liquid biocrudes [7].

A process that has received less attention is the use of $s\text{CO}_2$ as the solvent for liquefaction and extraction. This approach has the potential to produce high-quality biocrude extracts with lower metal and water content along with superior density, viscosity, and phenolic content [8]. The supercritical fluid state possesses advantageous found in both gas and liquid states. It can penetrate the reactants like a gas and has the higher density of a liquid. The lack of surface tension and low viscosity aide in the high diffusivity. Further, the solvent power of $s\text{CO}_2$ is strongly tied to its density which can be precisely controlled with temperature and pressure. It is non-polar and well suited to extract lighter biocrude fractions. Supporting economic scaling, it is easy to separate and recycle CO_2 . Lastly, the extraction step significantly improves quality through enhanced separation of the oil and aqueous phases.

1.3 Biomass

Biomass refers to material from living organisms and is generally associated with wood, leaves, straw, and seeds. Among the most complex molecules and central to the definition of lignocellulosic biomass is the lignin molecule. These large molecules are polymers of phenylpropane units [9]. An example of the structure is in Fig. 2 where the origins of many of the phenols in then end products can be seen.

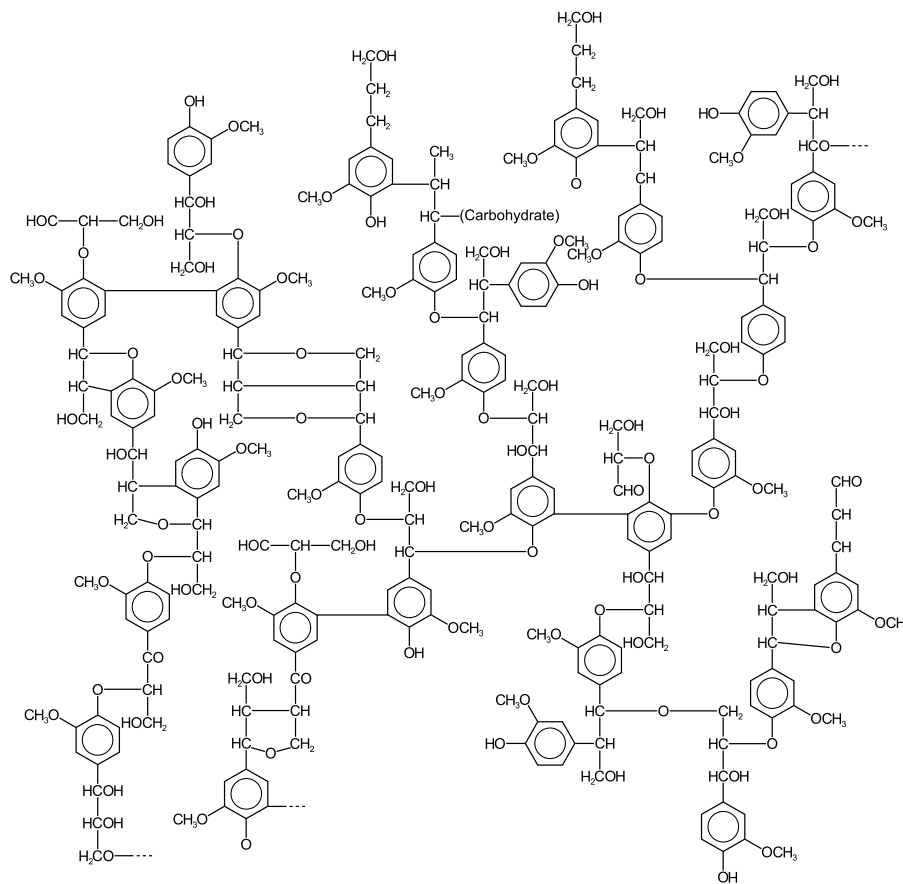


Fig. 2 Lignin Structure [10]

In addition to lignin, the biomass is comprised of cellulose and hemicellulose. Cellulose is the dominant component, making up just under half the dry mass of typical biomass. It is highly structured and cross linked. The cellulose builds up from microfibrils to large fibers that have high tensile strength and near zero solubility [9]. Hemicellulose also functions to support cell walls but contrast in that they are easily hydrolyzed by acids and are less polymerized. They typically represent closer to 20-30% of dry biomass [9].

1.4 Heating and Cooling rate

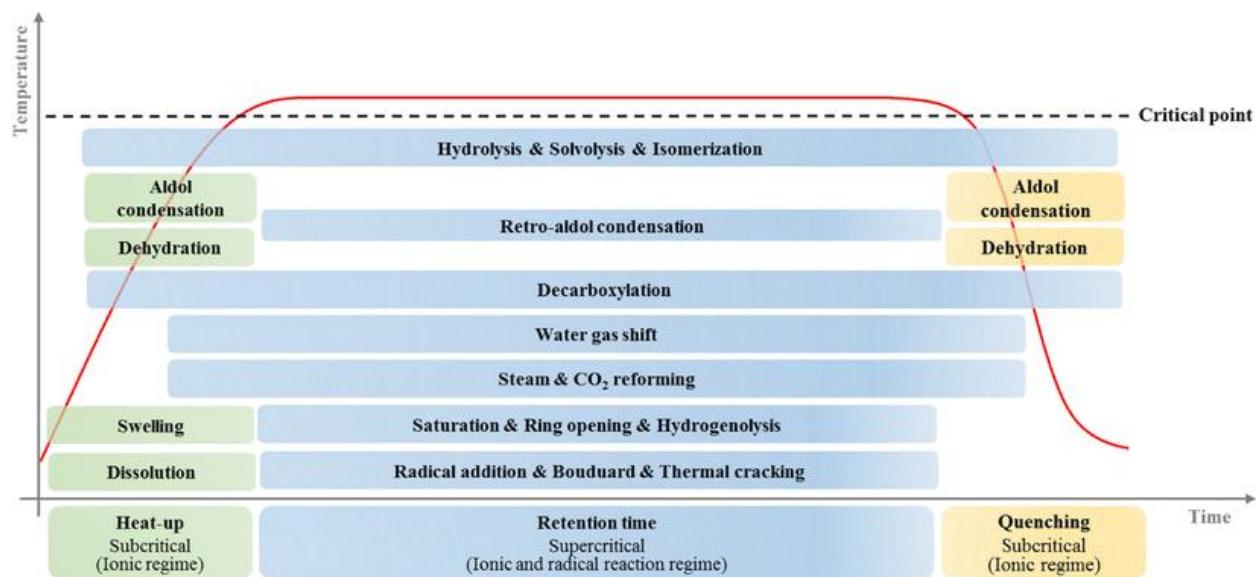


Fig. 3 Various Hydrofaction™ reactions depending on time and temperature [3]

The desired sCO₂ liquefaction reaction occurs above a threshold temperature. While the reaction is slightly different and can be at a lower temperature than hydrothermal liquefaction, there is a similar detriment from the transient temperature periods before and after the residence time. As seen in the work done by Jensen *et al.* [3], time spent in transition to the goal temperature supports several undesirable reactions, most notably dehydration. The dehydration period allows for the intermediate molecules to interact in condensation and repolymerization reactions which can create more solid residue and lower liquid yields. Therefore, it is important to the overall yield and quality of the process to heat and cool as rapidly as possible to mitigate dehydration.

1.5 Temperature and Residence Time

Wang *et al.* [11] evaluated the impact of temperature and residence time on pinewood liquefaction in sCO₂. They found that as the temperature increased, the solid residue yields also decreased but that the aqueous products and gas yield increased. Therefore, there exists an optimum temperature for biocrude yield. Wang *et al.* further found that for a given temperature,

there exists an optimum residence time where solid residue formation was at a minimum and biocrude yield is at a maximum. These findings are summarized in Fig. 4.

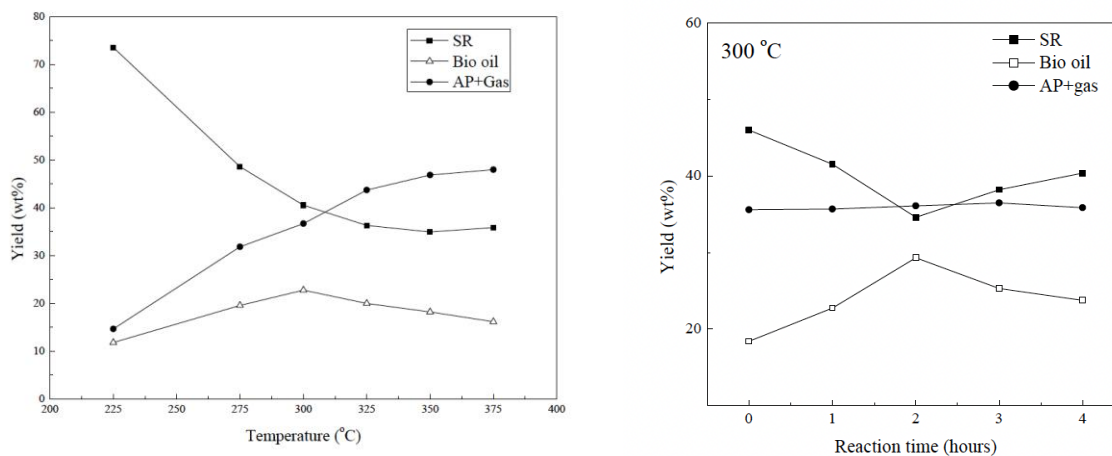


Fig. 4 Impact of temperature and residence time [11]

1.6 Near-critical Liquefaction Extraction (NILE) in sCO₂

Early work by Kiran et. al. established the viability of sCO₂ for both liquefaction and for extraction [12]. The extraction effectiveness was well established and performed in accordance with the greater field's expectations.

Reasonable yields of high-quality biocrude oil were successfully produced in a 100 ml small-batch reactor, validating the efficacy of the process. The previous work demonstrated that, under optimized temperature, pressure, and CO₂ density parameters, a catalyst is sufficient to enable the reaction in a sCO₂ environment. This had the potential to mitigate the complexity and costs associated with co-solvent supported reactions [13].

The advantage sought was the combination of the liquefaction and extraction processes. Exclusive reliance on sCO₂ as the solvent would simplify the process and reduce costs. It would also be advantageous for continuous flow operations due to the relative ease of CO₂ separation and recycling compared to solvents that are liquid at room temperature and pressure.

The group's prior work had not yet achieved comparable reaction performance at larger scales than the 100 ml reactor nor developed the combined liquefaction and extraction apparatus. The opportunity for continued research was focused on testing liquefaction at an order of magnitude greater scale, the development, fabrication, and testing of the combined process apparatus, and evaluation of the resulting biocrude yield and quality.

Chapter 2: Materials and Equipment

2.1 Materials

The biomass was pinewood supplied by the Idaho National Laboratory (INL). The as-received size distribution was evaluated using sieve analysis, the results of which are presented in Table I. Sieve stack was manually shaken for 10 min. Fine particle sizes were found to migrate significantly during combined liquefaction and extraction. This migration bypassed residence time in the reactor and contributed to clogging in the reactor - extractor connection. Thus, particles below 106 μm (No. 140 sieve) were rejected. Large particles were found to jamb the stirrer in the feeder and contribute to clogs between the feeder and reactor, thus particles above 710 μm (No. 25 sieve) were rejected. Based on the original size distribution, this maintained 94.5% of the mass while addressing experimental complications. The separated biomass was then oven-dried at 105 $^{\circ}\text{C}$ for at least 12 hours. Prepared biomass was stored with a desiccant to maintain negligible moisture content.

TABLE I. Mass Fraction of INL Pinewood

Size	Mass Fraction
<75 μm	0.0048
75-106 μm	0.0153
106-150 μm	0.0283
150-425 μm	0.2215
425-500 μm	0.4511
500-710 μm	0.2444
710-1000 μm	0.0248
1000-1180 μm	0.0044
1180-1700 μm	0.0040
>1700 μm	0.0013

All processes without a co-solvent utilized potassium carbonate as a catalysis at a 1:10 mass ratio to biomass except where specifically noted.

2.2 Equipment

2.2.1 Reactor

All of the liquefaction process were conducted in a nominally 1300 mL stainless steel (316L) vessel, hereafter the reactor, manufactured by Parr Instrument Company. The reactor had internal dimensions 3.25 inch diameter, 9.8 inch height and an assembled mass of 27.76 kg. It incorporated a magnetic stirrer with cooling jacket, a thermal well, a pressure relief safety valve, a fluid input valve with pressure gauge, an output port, and a straight through port capable of supporting $\frac{3}{8}$ in high pressure tubing that was used for both an additional thermal couple and biomass inflow. Two thermal well lengths were used, 8 in and 5 in. The reactor head was sealed to the body of the vessel via compression of a polytetrafluoroethylene (PTFE) seal enhanced with a silicon grease. The compression was achieved using eight lug nuts torqued to the manufacturer's recommendation.

2.2.2 Reactor Stirrers

A variety of stirrers were investigated. One incorporated four fins at the base of the reactor and a paddle to agitate components higher in the chamber. It additionally had a minor fan with the intent of disturbing fluid in the upper portion of the reactor; however, its effectiveness was likely negligible as it was not of an optimized fan geometry. This stirrer was generally ineffective at moving the fluid components.

This was replaced with a stirrer modeled off typical paint mixers. The spiraling arms extending from the center shaft expanded to the inside diameter of the reactor. The spiral was such that it displaced components downward in the reactor and was intended to bring all reaction

elements in close proximity. A 1.5 inch diameter fan was mounted high in the reactor volume to push fluids down. However, the compaction of solids at the base of the reactor caused high torque demands that would surpass the capabilities of the magnetic stirrer, resulting in slips.

The last stirrer assembled was entirely of purpose-built (commercial off the shelf) fans to maximize the fluid displacement while still adequately disturbing the solids. Two 3 in fans were mounted in the lower portion of the reactor with a counter flow fan at the bottom such that the fans on a common shaft worked to move fluids and solids towards each other. A 1.5 in fan was still used in the upper portion of the reactor to displace fluids towards the reactants in the lower volume.

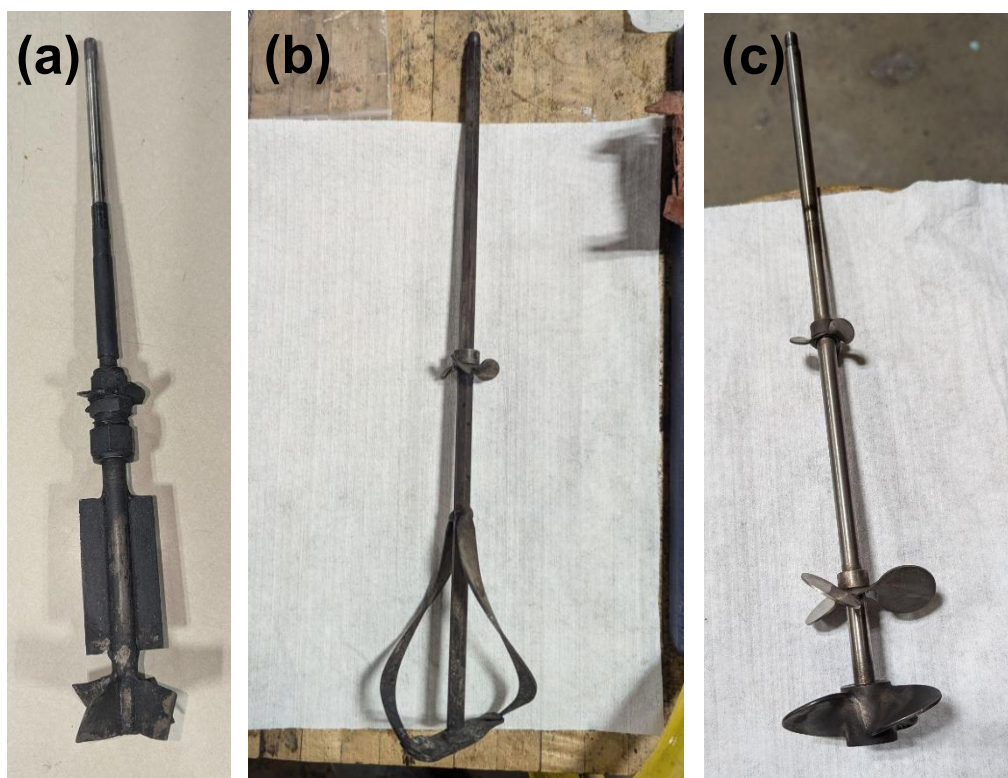


Fig. 5 Reactor Stirrers. (a) Paddle based. (b) Paint mixer based. (c) Counterrotating fans.

2.2.3 Feeder

Two vessels were used to feed biomass into the reactor at high pressures. The first was a 300 ml Swagelok 316L sample chamber with port dimensions of ¼ in NPT on either end and a concave transition to the openings. This vessel was ill suited for feeder function. Loading biomass through the ¼ in port was in excess of 60 min process for 50 g. Further, the concave internal transition was not suited for solid particle flow. Biomass would accumulate at the curve and provide sufficient bridging to prevent biomass at the center from exiting. The narrow internal diameter also made stirring impractical. This vessel was abandoned and replaced.

The second was a stainless steel (17-4PH) cylinder with a conical transition to the outlet at approximately 24° slope from the horizontal. The interior dimensions were 3 inch diameter and 9.5 inch height. The cylinder incorporated a full-diameter threaded closure that greatly improved loading process. The closure included a concentric port through which was passed a magnetic stirrer. An additional port through the cylindrical wall provided CO₂ input. Various agitators were investigated alongside various conical inserts of different angles. However, material limitations prevented use of the inserts under test conditions and an agitator was created to match the unmodified interior of the vessel. The agitator was crafted using Swagelok fittings, a central shaft of ⅛” copper that extended into the outlet fittings where it was hammered flat, and a ⅛” flexible stainless steel tube extending laterally to the interior wall then following the wall and cone until it intersected the center shaft at the outlet opening. The agitator was rotated at 500 steps per second or 150 rpm.

2.2.4 Collector (light fractions)

A 500 ml vessel rated up to 55 bar. The collector was typically at or near room temperature to condense light fractions. 40-50 bar of pressure enabled the ABPR to function more consistently.

2.2.5 Extractor (heavy fractions)

A 500 ml vessel rated up to 600 bar at 150 °C. Multiple input ports allowed for either preloading of products for extraction or to run continuous flow through the vessel wherein the lower temperature encouraged condensation of heavy fractions while maintaining the high pressure such that light fractions remained soluble in the sCO₂.

2.2.6 Automatic Back Pressure Regulator (ABPR)

A proportional-integral-derivative (PID) controlled high-precision, closed-loop fluid control system to dynamically maintain a consistent pressure at its inlet, regardless of flow.

2.2.7 Heater

Primary heat source was via U.S. Solid Induction Heating Systems, 16:1 turns ratio induction heater. It had rated maximum output power of 15 KW with a current range of 90 – 600 A. Input was single phase 220 V. Induction coil manually fabricated using copper tubing which incorporated active water cooling and completed four turns distributed vertically around the reactor.

To address potential heat loss from the bottom of the reactor and to increase temperature uniformity, an electric joule heater was added below the base of the reactor and energized concurrent with the induction heater.

2.2.8 CO₂ supply and pump

CO₂ was supplied from a compressed cylinder with siphon tube supplied via Airgas. The liquid CO₂ was precooled to below 10 °C in a heat exchanger using 50/50 glycol water chilled to between -20 °C and 0 °C. The same chilled water was supplied to heat exchangers at the pump. The pump itself was a Core Separations model SFXP5S-689 and composed of parallel displacement pumps, single piston each. The rated maximum flow was 60 g/min and a maximum

pressure of 689 bar. Check valves on either side of the piston were found to jam under unfavorable conditions with suspected dry ice formation the culprit when pressures dropped too low. Therefore, care was taken to modulate the flowrate through the check valves when charging the downstream components up to CO₂ cylinder pressure prior to pumping. The elevated pressure liquid CO₂ was then passed through a preheater at 100 °C and emerged either as vapor or super critical depending on the pressure.

2.2.9 Fully assembled test apparatus

The fabrication of the combined liquefaction – extraction test apparatus was a significant achievement of this work. In the following series of figures the equipment is shown in its assembled arrangement.

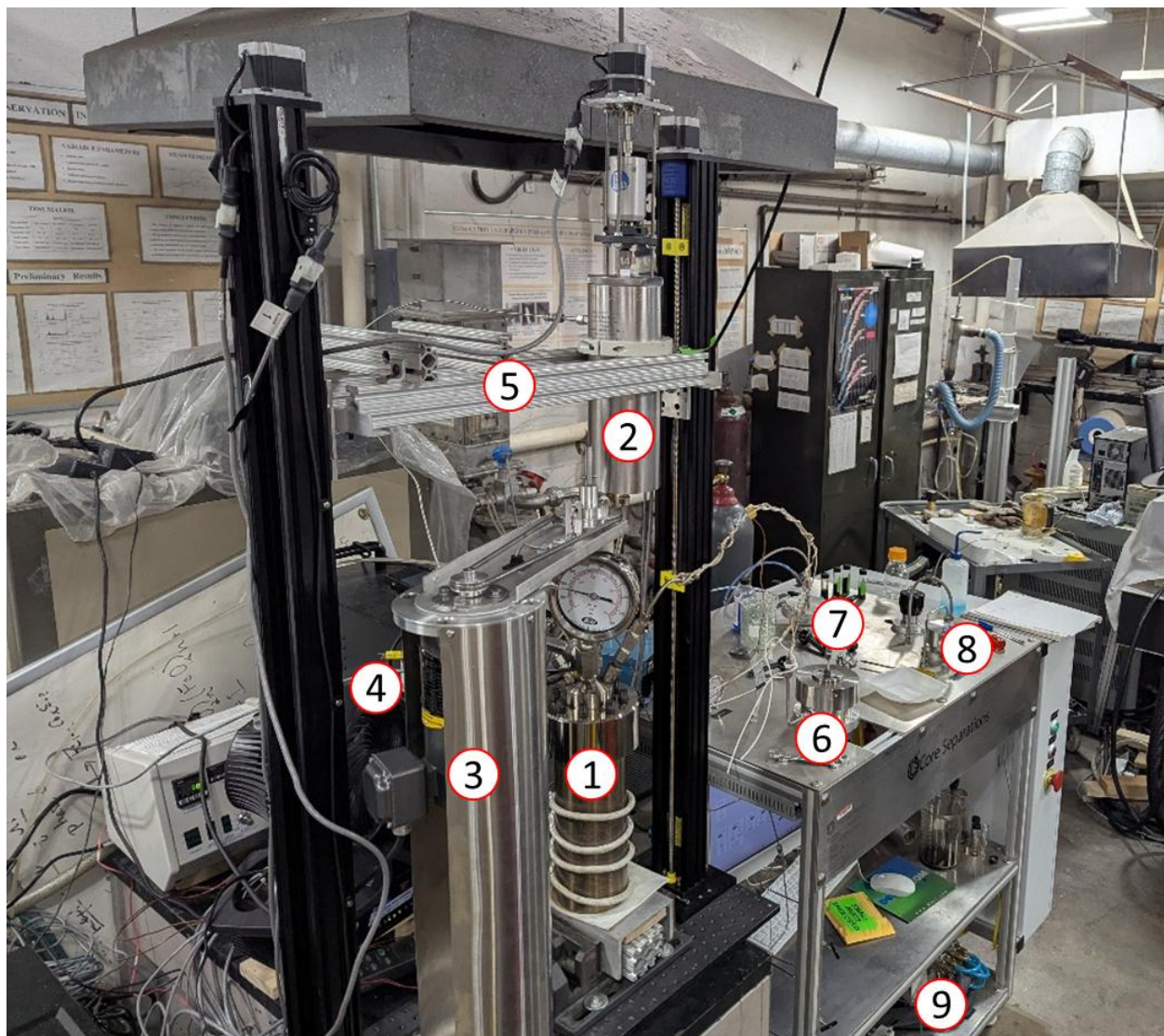


Fig. 6 Combined liquefaction-extraction, before addition of heated base. (1) Reactor. (2) Feeder. (3) Reactor stirrer motor. (4) Cooling fan. (5) Movable feeder gantry. (6) Extraction vessel. (7) ABPR. (8) Collector vessel. (9) CO₂ pump



Fig. 7 Reactor with heated base plate added

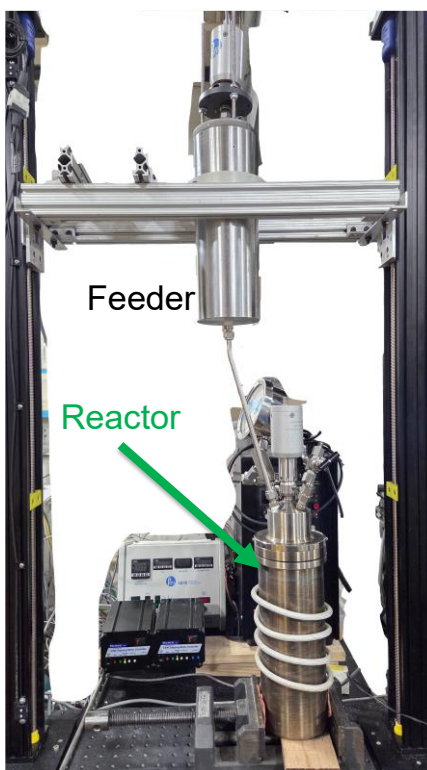


Fig. 8 Feeder and reactor connected with 3/8 in high pressure tubing

Chapter 3: Procedures

Three broad categories of process were utilized. These were a concurrent liquefaction and extraction, a batch reaction with direct extraction, and a batch reaction with separate extraction.

3.1 Concurrent liquefaction and extraction

The biomass was prepared as described in Materials and when in use, the catalyst was mixed with biomass prior to loading into either the reactor or the feeder. The feeder was used to improve heating time of the biomass by separating the sensible heating of the reactor body from the heating of the biomass. In isolated testing at atmospheric conditions, it was found that the biomass would not flow from the feeder without active agitation via the stirrer. It was also found that implementation of a ball valve in the connection between feeder and reactor consistently caused clogging. The interior diameter within the valve was slightly larger than the interior diameter of the tubes. The abrupt transition provided a ledge to capture particles, which quickly developed into a bridge obstructing the flow completely. Therefore, a valve at this location was not utilized.

In feeder supported reactions, the biomass was loaded into the feeder and the reactor volume was empty at apparatus assembly. CO₂ was fed into both the feeder and reactor until pressure reached CO₂ cylinder level and then fed only through the feeder. The induction heater increased temperature concurrent with CO₂ pumping until both parameters reached the test conditions. The agitator in the feeder was then activated and ran for a minimum of 20 minutes. To mitigate clogging in the tube between feeder and reactor, it was routinely subjected to mechanical percussion. The extraction time started after the 20 minutes of feeding which was believed to provide excess time beyond the benchmark established in atmospheric tests.

In reactions without the feeder, biomass was added directly to the reactor prior to closing the reactor head and the port for the feeder connection was either closed or later used for an additional thermocouple. The same approach was followed for the preload of CO₂ and then the reactor heated at full rate. The extraction time counted from when the reactor's temperature as determined at the thermal well reached the test conditions.

In both cases, the outflow from the reactor was open for the duration of the experiment. The tube connecting the reactor to the extractor was heated with a resistance cable to mitigate condensation and clogging. The temperature in the extractor was maintained at 100 °C to condense heavy fractions. Solid particulates carried by the flow were routinely discovered in the extractor, particularly in feeder supported reactions. A filter at the extractor's outlet mitigated further intrusion. The flow continued to the ABPR followed by the vaporizer and finally the collector maintained at approximately 40-55 bar and 22-40 °C. A manual pressure regulator on the outlet maintained the differential before the remaining flow vented to atmosphere.

3.2 Batch Reactions

After initial combined liquefaction-extraction tests provided marginal results, confirmation of the reaction conditions was necessary. To evaluate the liquefaction reaction specifically, a series of batch tests were conducted in varying degrees of isolation from the rest of the apparatus. The overall objective was to determine the optimum liquefaction conditions for the specific reactor in use and then reintroduce the integrated steps. Based on the work done by Wang *et al.* [11] discussed previously and results in the smaller reactor done by Burra *et al.* [13] the presumed conditions were 300 °C, 300 bar, 10% by weight catalyst, and moderate stirring. These parameters were adjusted and the yield by mass of biocrude was calculated to determine the relative impact. Generally, the outputs collected were the mass of char and liquids. The liquid was separated into

aqueous products and oils. On a mass balance basis, the residual was a combination of gasses and assumed losses. Except where specifically noted, the biomass was mixed with the catalyst and loaded directly into the reactor before assembly. The reactor was then sealed, moved to the induction coil, and all ports connected. When purging was implemented, either gaseous N₂, Ar, or CO₂ was used. The outflow was then closed and CO₂ was fed into the reactor until it reached 50 bar. The reactor was then pre-heated to 50 °C achieving a stable enough state to load the desired density of CO₂. Attempts at lower energy states were prone to inconsistent results. Using NIST data, the corresponding pressure at 50 °C that would result in the desired reaction conditions was determined. CO₂ was then pumped into the reactor to achieve the starting pressure. The heating output was then maximized to reach the test parameters in minimal time. As the target temperature approached, typically within 40 °C, the output of the induction heater would be manually reduced. This continued step wise to mitigate transient overshoot. Once the system was stabilized at the target temperature, continuous monitoring and adjustment was necessary to maintain the target temperature and generally lower power levels were required as the test progressed.

At the conclusion of the residence time, all heating elements were turned off and an axial-flow fan was used to increase the convective cooling. Stirring continued throughout the cooling process to improve temperature uniformity. Cooling was allowed to continue until the temperature fell below 30 °C to ensure the CO₂ was no longer supercritical.

3.3 Acetone Extraction

In many tests, acetone was used to separate the liquids from the solid residues, particularly after the batch reactions. The oils were filtered to remove residual small solids and then transferred to a 1 L round-bottom flask. A rotary evaporator made by Cole-Parmer was then used to then separate the acetone from the oils, generally at atmospheric pressure.



Fig. 9 Rotary Evaporator

3.4 sCO₂ Extraction

The two varieties of sCO₂ extraction were directly from the liquefaction reactor and from the extraction vessel after transferring the liquefaction products between vessels. In the direct from reactor procedure, whether the liquefaction was batch or combined, the general process closely aligned with the flow detailed in section 3.1 above. The distinction for batch reactions was that the reactor would be cooled to and maintained at 100 °C and then the continuous flow of sCO₂ into the reactor increased the pressure back to extraction conditions of approximately 300 bar. The outlet and downstream flow were as described in section 3.1.

When extracting from the extraction vessel, the reactor would be cooled to below 30 °C as described in section 3.2 and then gases vented to atmosphere. Once depressurized, the reactor was opened and the liquefaction products could be transferred between vessels. Liquids would be soaked into cotton to aide suspension in the extraction vessel and avoid counter flow as a result of gravity moving the liquid through the filter on the CO₂ inlet.

3.5 Process Flow

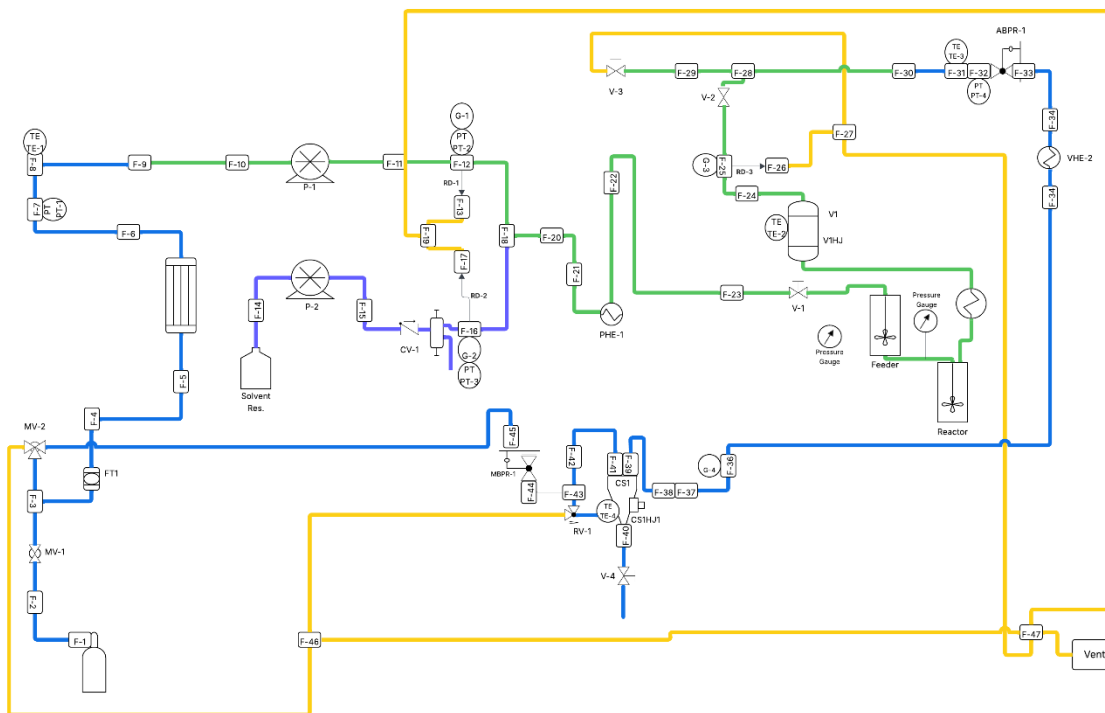


Fig. 10 Process flow diagram for integrated liquefaction-extraction

The process flow diagram in Fig. 10 provides a schematic view of the overall system. The diagram visually represents the primary flow paths and equipment required for both the continuous and batch operating modes. Key components include the liquefaction reactor, the CO₂ pump, the feeder, the extraction vessel (V1), the collection vessel (for light fractions, CS1), the solvent reservoir (used for supplementary co-solvents), and the lines dedicated to the pressurization and delivery of sCO₂. The placement of various control valves (e.g., CV-1, MV-1/2), pressure transmitters (PT), and temperature elements (TE) highlights the precise control and monitoring capabilities necessary for manipulating the fluid properties of sCO₂. This level of control is critical for tuning the solvent power and achieving the selective separation detailed in previously. The

arrangement also shows the mechanisms for product recovery and depressurization through the extraction and separation lines, allowing for efficient separation of the biocrude from the solid residue and the recyclable CO₂ stream.

Chapter 4: Results

4.1 Biocrude Yield

There was not a single parameter that performed appreciably well as an independent variable and therefore the batch results are aggregated for relative comparison here. Tests are identified with a shorthand description and notable results are reviewed in detail. Absence of a value indicates data the measurement was not made for that item.

The vast majority of the liquid yield mass results were within one standard deviation suggesting that stability of the reaction within the evaluated parameters. Notable exceptions were tests identified as Resistive Heating (decrease in liquid yield, -1.148σ), 130g Biomass (increase, 1.727σ), Argon Environment (increase, 4.675σ), 50g Batch w/ CO₂ extract (decrease, -1.970σ), Rapid Cooling (decrease, -1.606σ), and hot plate (decrease, -1.515σ).

The highest oil yields were from the expected ideal conditions of 300 °C, 300 Bar, and 120 min residence time. There was also a stronger result when the biomass to CO₂ ratio was higher, in the range of 1:3 whereas the majority of the tests where in the range of 1:7.

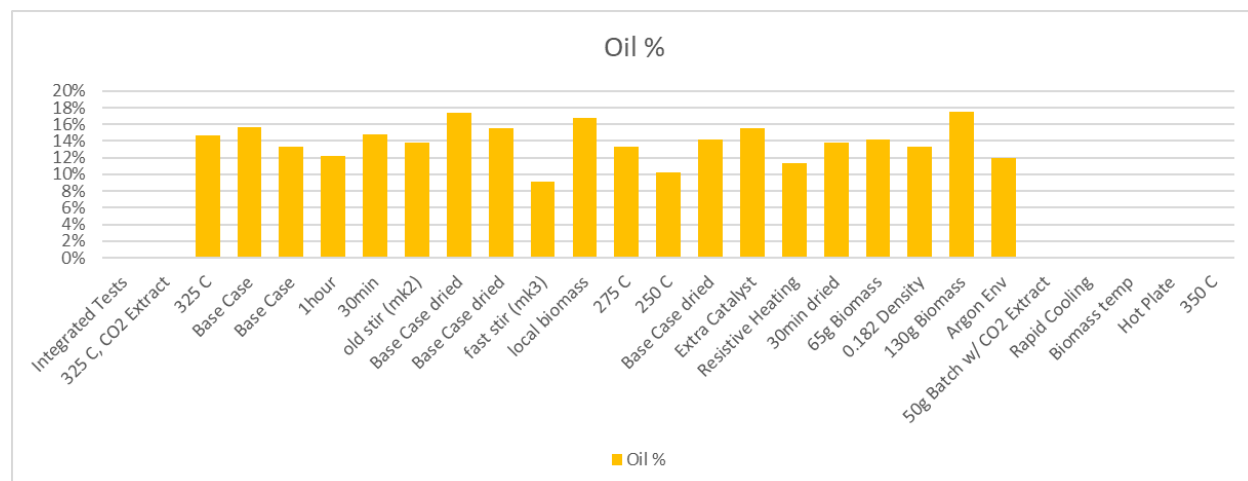


Fig. 11 Oil (biocrude) yields

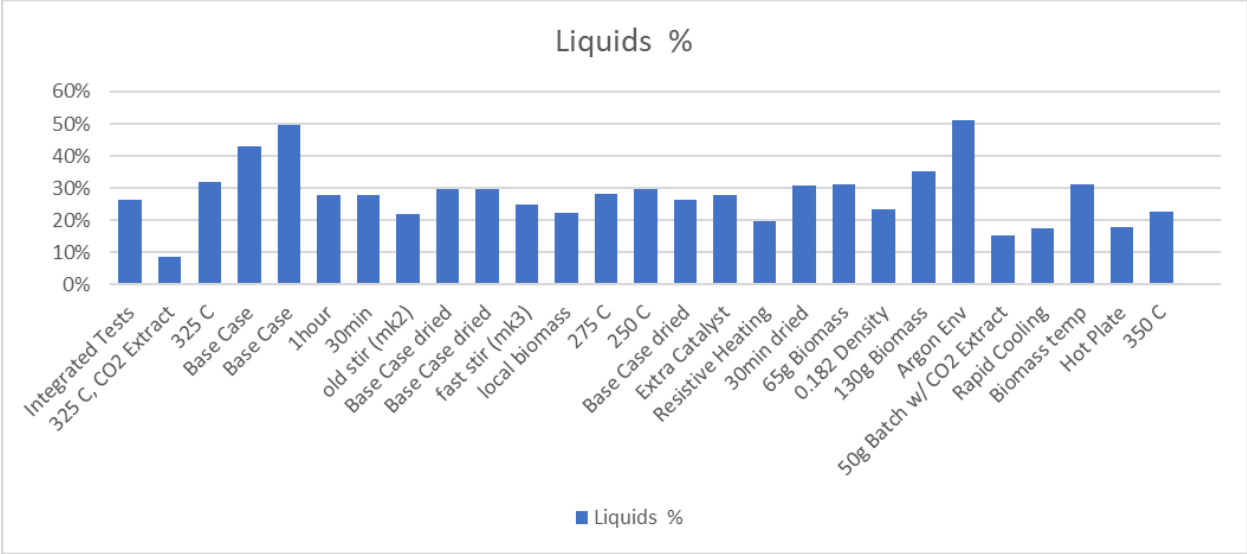


Fig. 12 Total liquids yields

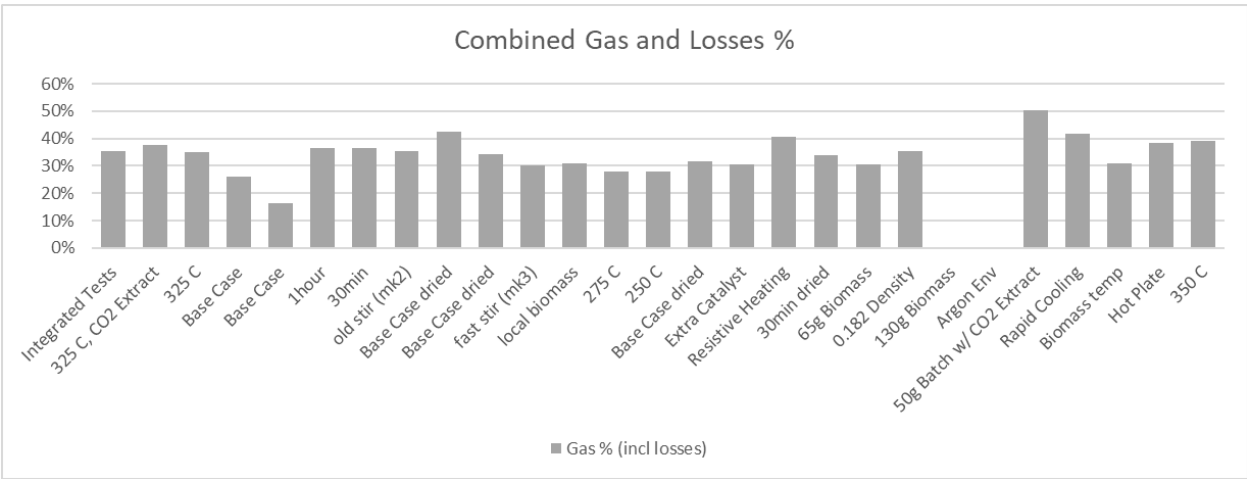


Fig. 13 Combined gas yields and losses. These values are calculated by subtraction of solids and liquids.

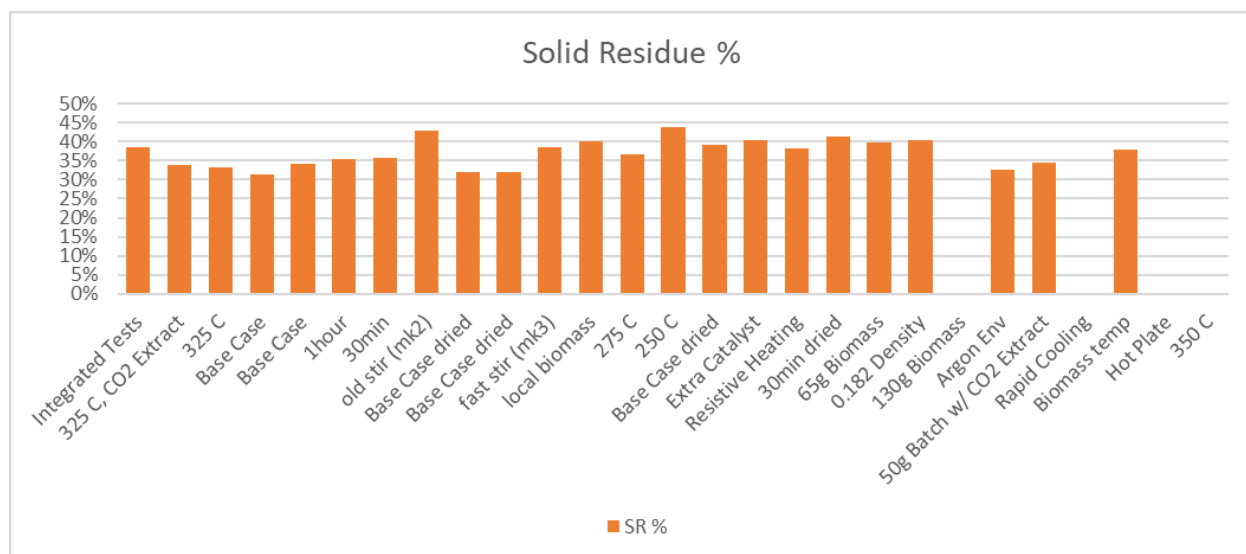


Fig. 14 Solid residue yields

The transition to dried biomass was done concurrent with the old stir (mk2) test and maintained thereafter. The liquid yield was therefore decreased from the reduction of entrained water. Additionally, more biomass was available for the reaction as the water mass was not offsetting the input. Generally, the total liquid yield was a leading indicator of the test results. When initially collected the aqueous products and oils were well mixed. Left to separate by gravity, within the short term the oils would generally exhibit lower density than the aqueous products but after 2-3 days the arrangement would reverse. As more of the oils settled out of mixture with the aqueous products the average density decreased and eventually the aqueous products would float to the top. The aqueous products when acetone extraction was used generally carried a yellow hue, likely from the presence of phenols. The aqueous products from sCO₂ extraction were much clearer as a result of the separation efficiency of the sCO₂.

The typical heating timeframe with the induction heater was in the range of 12-18 min with variability attributed to the manual control of the output power in pursuit of the specific test parameter. To evaluate if the lack of surrounding insulation and uneven heating caused by the induction coil were detrimental, a test was performed using the Parr supplied electric joule heating

furnace matched to the reactor. This furnace includes ceramic insulation and heating elements surrounding the vertical face of the reactor from bottom to below the collar assembly. The heating time was significantly longer, taking 1 hr 38 min to reach the test parameter of 300 °C. Both the total liquid yield and the oil yield were notably lowered, with oil yield falling to just 11.3%. The faster heating rate of the induction heater mitigates time in the dehydration and hydrolysis temperature ranges, ultimately supporting higher oil yields.

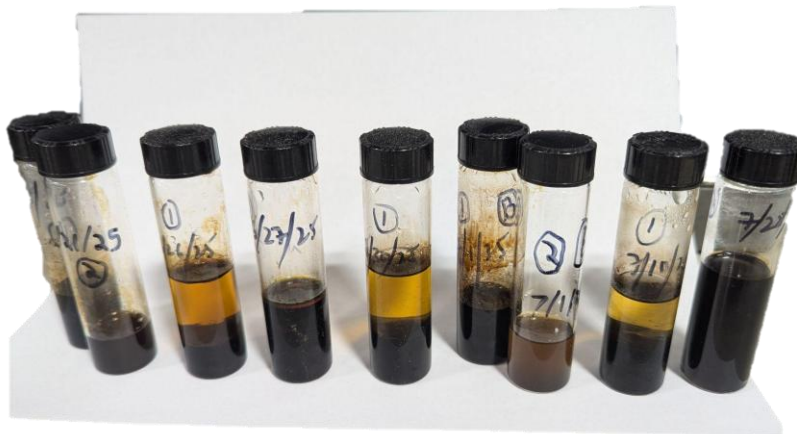


Fig. 15 Representative liquid extracts showing oils and aqueous products



Fig. 16 Immersion cooling test using ice water bath

To evaluate if the extended cooling time was contributing to the production of water and lower oil yield a rapid cooling test was performed. Rather than the forced air convection cooling, the reactor was immersed in an ice and water mixture. This improved the cooling performance to below 100 °C from a typical time of 30 min to 2:20 min:sec and to below 30 °C from 100 min to 7 min. Aqueous products were qualitatively observed to be minimized. However, the total liquid yield was reduced to 17.3% and the reduction in water yield did not translate to an increase in oil yield, thus the additional complexity of the immersion cooling was not beneficial.



Fig. 17 High aqueous product yield from argon only environment

To evaluate the effect of pressure alone, distinct from the presence and density of CO₂, a test was conducted in an Argon environment. No CO₂ was used during the liquefaction. The pressure at 300 °C was 300 bar to align with the typical conditions. The reaction produced a significant number of aqueous products which caused the total liquid yield to surpass 51% or 4.675 standard deviations above the mean. However, the oil yield was only 11.93%. Thus, the sCO₂ is a beneficial solvent for the reaction.

4.2 Composition of oil product

Two representative sample were analyzed using Gas Chromatography-Mass Spectrometry (GCMS). The analysis was done with Thermo Scientific Trace 1300 Gas Chromatograph. The first sample aligned with the base case assumption on test parameters, 300 °C, 300 bar, 120 min residence time, and other factors as discussed. This test had among the highest oil yield at 17.42%.

The other analyzed sample was from a test that matched the former in parameters except for a 30 min residence time. The yield was 13.83%, although lower was still among the best results in this study. Given the significant operational and cost benefits of a one-quarter residence time, if the quality of the oil was comparable then the economic benefit at scale would favor the shorter residence time.

The samples were prepared for GCMS using NREL's Laboratory Analytical Procedure for Quantification of Semi-Volatile Oxygenated Components of Pyrolysis Bio-Oil by Gas Chromatography/Mass Spectrometry (GC/MS) [14]. The procedure includes the introduction of internal standards to provide a basis to estimate the weight fraction of the detected components. The peaks were analyzed for likely components and labeled. Figs. 18-22 provide the composition of the two samples displaced in the Total Ion Chromatogram.

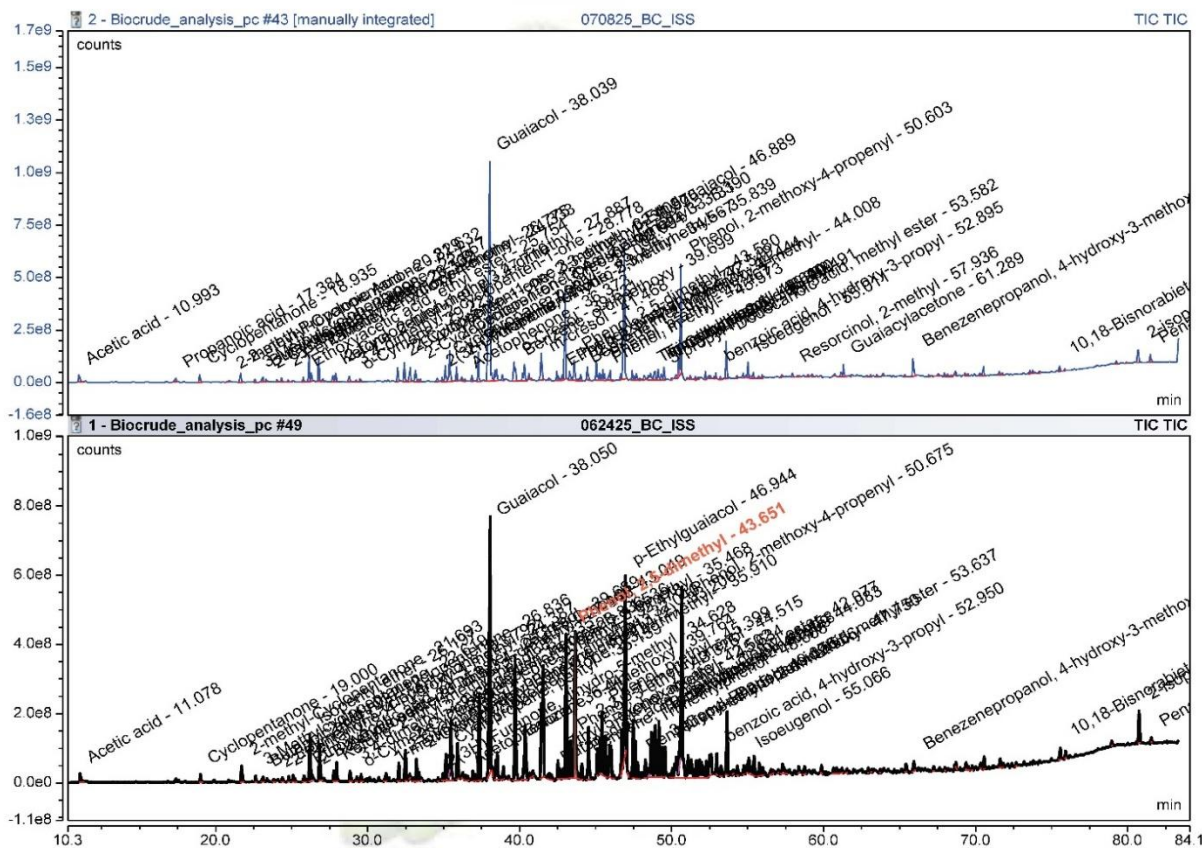


Fig. 18 Full plot of Total Ion Chromatogram, upper samples is 30 min and lower sample is 120 min residence time.

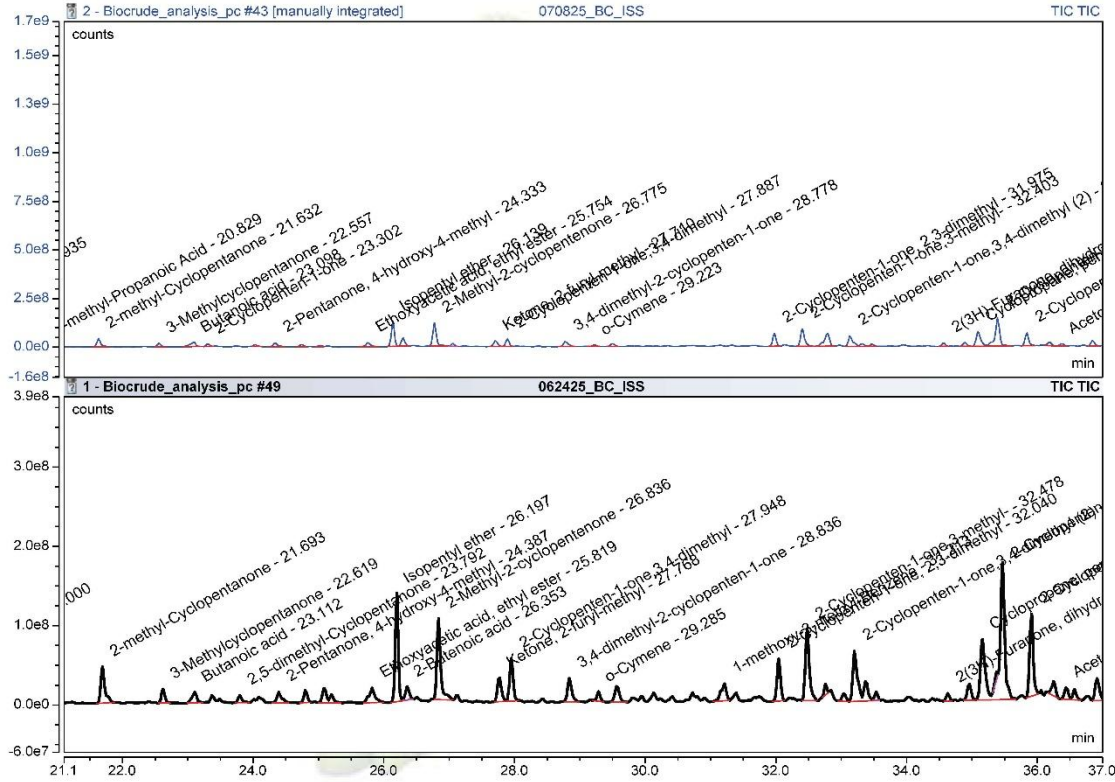


Fig. 19 Total Ion Chromatogram for retention times between 21-37 min, upper samples is 30 min and lower sample is 120 min residence time

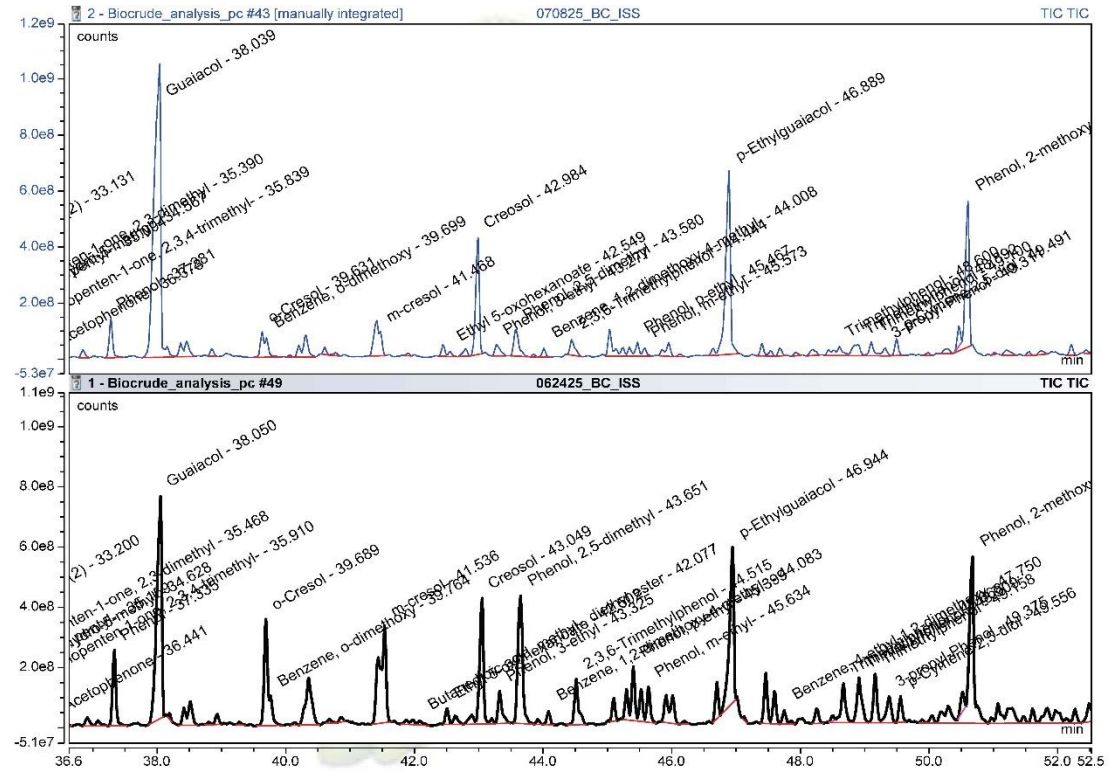


Fig. 20 Total Ion Chromatogram for retention times between 37-52 min, upper samples is 30 min and lower sample is 120 min residence time

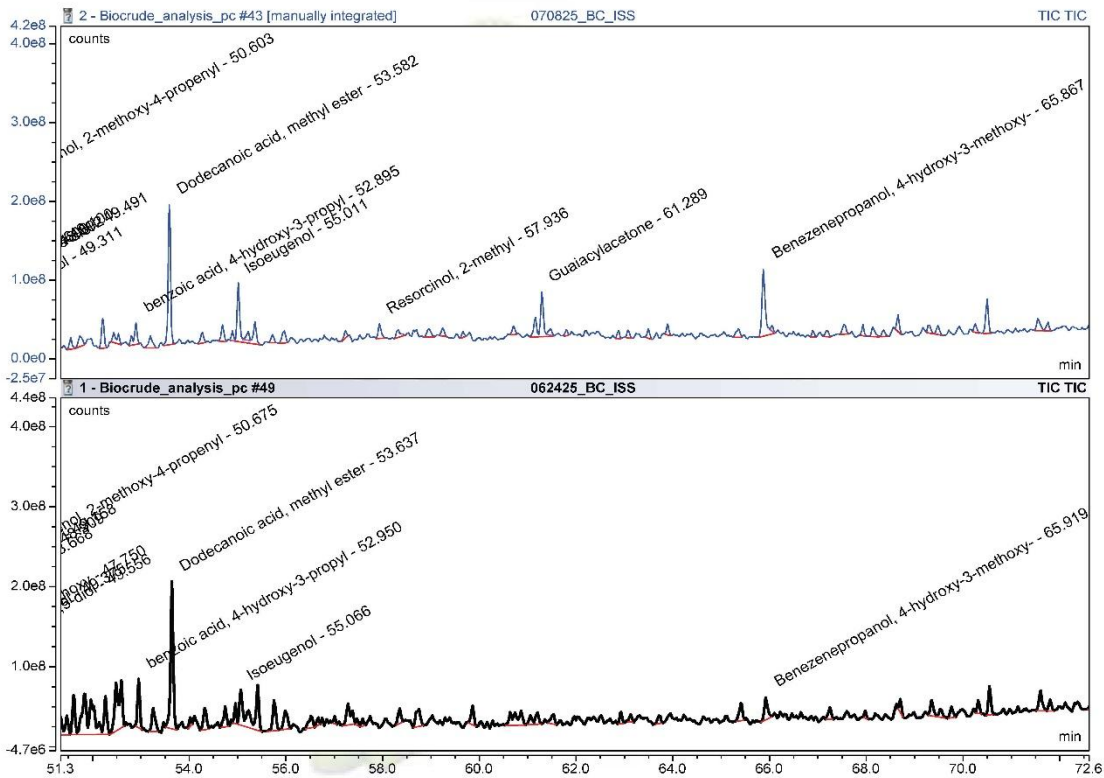


Fig. 21 Total Ion Chromatogram for retention times between 52-72 min, upper samples is 30 min and lower sample is 120 min residence time

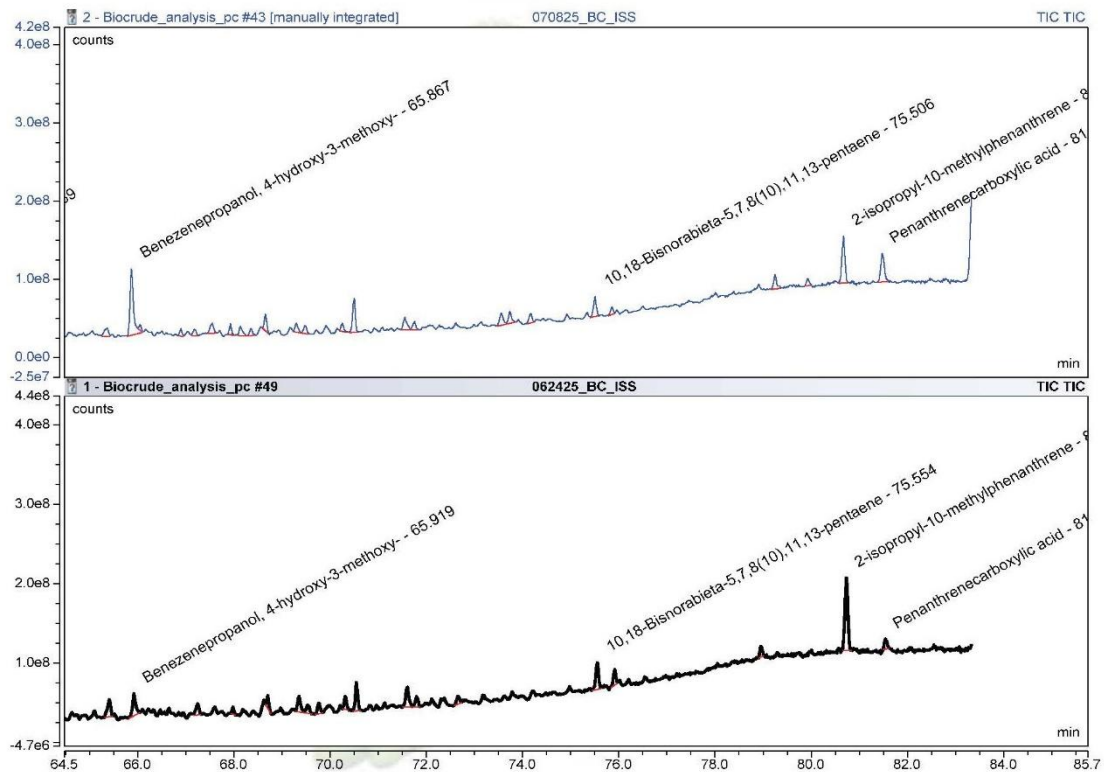


Fig. 22 Total Ion Chromatogram for retention times between 65-84 min, upper samples is 30 min and lower sample is 120 min residence time

Effort was made to align the vertical axis for each of the chromatogram figures; however, it is important to note that visual comparison between the perceived heights and areas of the peaks is not sufficient to infer relative mass fractions. Representative components were analyzed relative to their respective internal standard across an average of three samples per test result. The calculated relative areas are provided in Fig. 23.

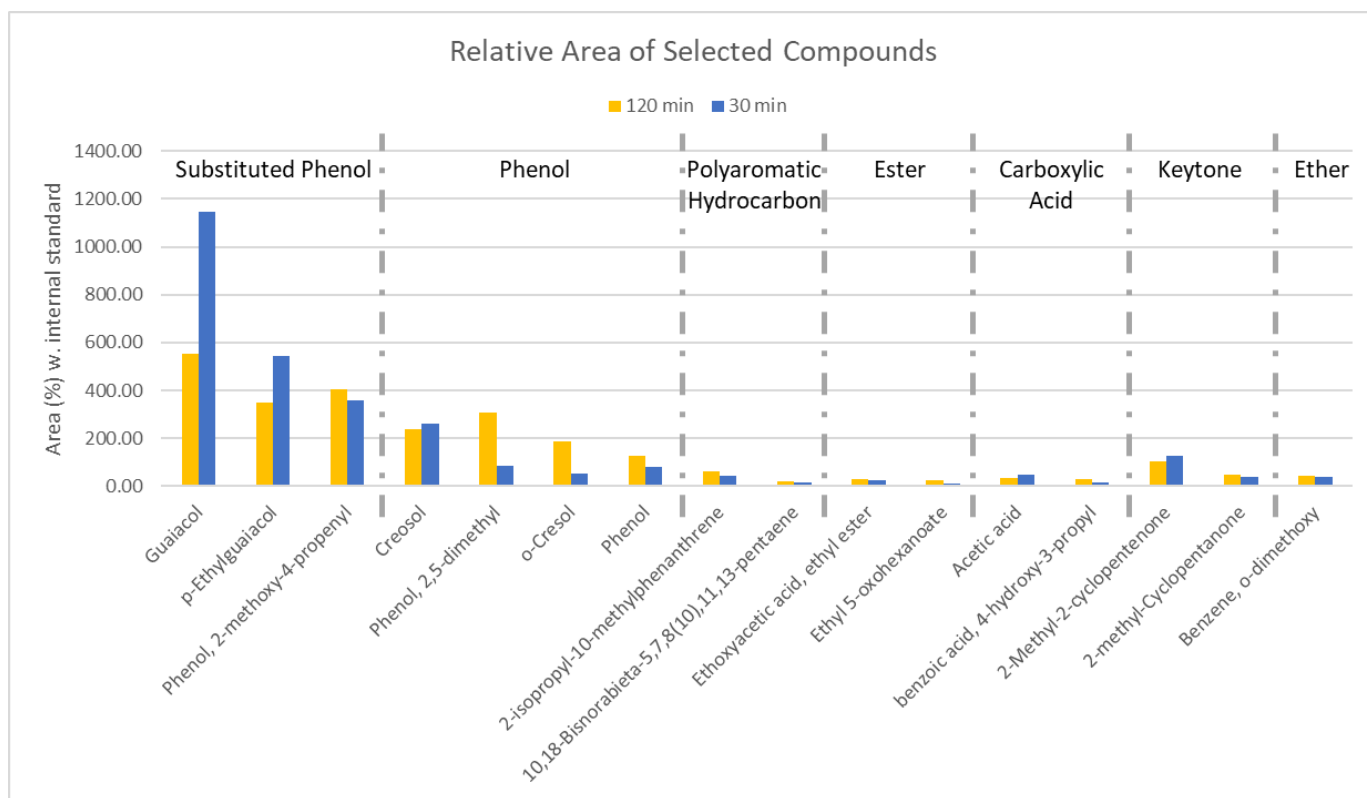


Fig. 23 Relative Area of Selected Compounds

As shown in the above figure, a guaiacol dominates the single compound production. Further, there was twice the relative area in the 30 min test than the 120 min test. There was also a greater relative area in the 30 min test for the p-Ethylguaiacol. The 120 min test did have a higher result for 2-methoxy-4-propenyl-Phenol. Overall, across the substituted phenols the 30 min test

had 1.56 times the relative area. For the phenols combined the 120 min test had 1.80 times the relative area. For 2-Methyl-2-cyclopentenone, the 30min edged out by 1.07 times. For the remaining compound categories, relative area was significantly less, therefore while the proportional difference was still present, it is near negligible given the assumed marginal weight percentage of the original product. These results support the inference that the longer residence time provides for decomposition after the primary depolymerization, breaking down the substituted phenols into simpler compounds. Further studies should evaluate the impact of the relative ratios on the viable as a biocrude and optimize the reduction in production time against any reduction in biocrude quality.

4.3 Cosolvent introduction

In order to overcome the stagnant oil yield despite the altered parameters, a more fundamental shift was investigated. A water and ethanol (50/50 wt%) cosolvent was introduced at a 5:1 combined solvent-to-biomass ratio. This improved oil yield from under 20% when only sCO₂ to above 60%, along with improved biomass conversion. Both water and ethanol aided in a solvent role and in a heat transfer role. In addition to direct solvent roles in depolymerization, distribution, and contact of the biomass, the ethanol acted as a capping agent for esters and formaldehyde. Combined, this dramatically decreased the solid residue yield, to below 2% in some instances. The balance shifted to a liquid yield, thus the strong yield results. For the thermal perspective, the specific heat of sCO₂ is fairly low, in the vicinity of 1.3 J/(g*k), and thermal conductivity at only 0.0498 W/(m*k) according to NIST data. This provided a high resistance pathway for the heat transfer from the reactor walls to the biomass. The contact area between the biomass and the reactor walls is quite small due to the particle size and the biomass itself has poor thermal conductivity, therefore direct conduction is limited. The presence of the water and ethanol greatly

increased convective heat transfer, which reduces the time spent in the dehydration temperature zone during heating.

The phenols produced by the liquefaction reaction have the potential to serve a similar function as the ethanol cosolvent. By recycling the aqueous products, the need for ethanol recovery or additional ethanol input may be reduced. If the oil yield and the quality are not adversely impacted by the decrease in ethanol through subsequent recycling, this presents a promising path towards economic viability.

Chapter 5: Conclusions and Future Work

The global reliance on finite petroleum resources and the persistent demand for liquid hydrocarbons underscore the need for sustainable aviation fuel (SAF) derived from renewable feedstocks. This thesis investigated the application of sCO₂ in a combined liquefaction and extraction system for biocrude production from pinewood.

The experimental work successfully utilized a novel integrated system to demonstrate the potential for process intensification, operating across temperatures of 250–350 °C and 200-300 bar. A critical finding was that the overall combined process is primarily limited by the liquefaction reaction. However, rapid parameter screening in batch reactor setups confirmed that the sCO₂ system offers distinct advantages in extraction, separation, and integrated process efficiency should the liquefaction portion be improved. The resulting sCO₂ extracted biocrude exhibited favorable characteristics and pending further analysis is suited for replacement of petroleum based crude oil supply to refineries. The inherent ease of separating and recycling the CO₂ solvent further supports the economic viability of this approach by mitigating costly solvent recovery steps required in conventional methods.

Future research should focus on optimizing the NILE (Near-critical Liquefaction Extraction) process to maximize biocrude yield while maintaining high product quality. The most promising path forward is the development of a cosolvent strategy to enhance the solubility and conversion of the biomass within the sCO₂ environment.

Initial studies should continue the evaluation of an ethanol-water cosolvent to investigate its effect on biomass conversion rates and the resulting biocrude composition. This will establish a performance baseline for solvent-assisted liquefaction within the supercritical regime.

Following the ethanol baseline, research should transition to replacing external cosolvents with aqueous products generated during the liquefaction reaction. This method promotes material efficiency and reduces external solvent costs, moving the process closer to self-sustainability and maximizing resource utilization. Should the product phenolics not be sufficient to maintain yield and quality, highly efficient ethanol recovery and recycling innovations will be necessary for the process to scale.

Ultimately, the NILE system must be transitioned from the current bench-scale configuration to a larger, continuous processing system. This involves engineering improvements to the mechanical feeding system and optimizing reactor volume to enable handling a significantly greater throughput of biomass, proving the pathway toward industrial scalability for high-volume sustainable fuel production.

References

- [1] Lawrence Livermore National Laboratory. (2024, Oct.). *Estimated U.S. Energy Consumption in 2023: 93.6 Quads*. [Online Diagram]. Available: <https://flowcharts.llnl.gov/sites/flowcharts/files/2024-10/energy-2023-united-states.pdf>
- [2] J. Holladay, Z. Abdullah, and J. Heyne, "Sustainable Aviation Fuel: Review of Technical Pathways," U.S. Dep. Energy, Washington, D.C., USA, Rep. DOE/EE-2041, Sep. 2020. doi: 10.2172/1660415.
- [3] C. U. Jensen, J. K. R. Guerrero, S. Karatzos, G. Olofsson, and S. B. Iversen, "Fundamentals of Hydrofaction™: Renewable crude oil from woody biomass," *Biomass Conversion and Biorefinery*, vol. 7, no. 4, pp. 495–509, 2017.
- [4] A. V. Bridgwater, "Review of fast pyrolysis of biomass and product upgrading," *Biomass and Bioenergy*, vol. 38, pp. 68–94, Mar. 2012. doi: 10.1016/j.biombioe.2011.01.048.
- [5] M. Usman, S. Cheng, S. Boonyubol, and J. S. Cross, "From biomass to biocrude: Innovations in hydrothermal liquefaction and upgrading," *Energy Conversion and Management*, vol. 302, Art. no. 118093, Jan. 2024. doi: 10.1016/j.enconman.2024.118093.
- [6] M. Rafati et al., "Techno-economic analysis of production of Fischer-Tropsch liquids via biomass gasification: The effects of Fischer-Tropsch catalysts and natural gas co-feeding," *Energy Conversion and Management*, vol. 133, pp. 153–166, Feb. 2017. doi: 10.1016/j.enconman.2016.11.051.
- [7] A. Funke and F. Ziegler, "Hydrothermal carbonization of biomass: A summary and discussion of chemical mechanisms for process engineering," *Biofuels, Bioproducts and Biorefining*, vol. 4, no. 2, pp. 160–177, Mar. 2010.
- [8] Montesantos N, Nielsen RP, Maschietti M. *Industrial & Engineering Chemistry Research* 2020 59 (13), 6141-6153
- [9] Sjöström E (1993) *Wood chemistry: fundamentals and applications*, 2nd edn. Academic press, San Diego ISBN 9780080925899
- [10] http://upload.wikimedia.org/wikipedia/commons/e/ee/Lignin_structure.svg.
- [11] Y. Wang, H. Wang, H. Lin, A. Pelletier, Y. Zheng, and K. Li, "Liquefaction of Pinewood in Supercritical Carbon Dioxide (SCCO₂)," *Current Organic Chemistry*, vol. 17, no. 15, pp. 1596–1603, 2013. doi: 10.2174/13852728113179990069.
- [12] K. R. G. Burra, M. Sahin, Y. Zheng, and A. K. Gupta, "Near-Critical CO₂-Assisted Liquefaction-Extraction of Biomass and Wastes to Fuels and Value-Added Products," *Journal of Energy Resources Technology*, vol. 146, no. 1, Art. no. 011801, Jan. 2024. doi: 10.1115/1.4063813.

[13] K. R. G. Burra et al., "Effect of Operational Parameters on Supercritical CO₂ Assisted Liquefaction of Pinewood," presented at the ASME 2025 19th Int. Conf. on Energy Sustainability, Westminster, CO, USA, July 8–10, 2025, Paper ES2025-157794. doi: 10.1115/ES2025-157794.

[14] E. Christensen, J. Ferrell, M. V. Olarte, and A. B. Padmaperuma, "Quantification of Semi-Volatile Oxygenated Components of Pyrolysis Bio-Oil by Gas Chromatography/Mass Spectrometry (GC/MS): Laboratory Analytical Procedure (LAP)," National Renewable Energy Laboratory (NREL), Golden, CO, USA, Tech. Rep. NREL/TP-5100-65889, Mar. 2016.